Lifetime measurements and deformed states in ^{41}Ca†

S. L. Tabor, K. C. Young, Jr., D. P. Balamuth, and R. W. Zurmühle
Physics Department, University of Pennsylvania, Philadelphia, Pennsylvania 19174
(Received 22 May 1975)

The Doppler-shift attenuation method has been applied to measure the mean lives of levels in ^{41}Ca. States were populated using the ^{40}Ca$(d,p)^{41}$Ca reaction at $E_d = 3$ MeV and protons emerging from the reaction were detected near 180° relative to the beam. γ rays were detected in coincidence with the protons using a 65 cm^3 Ge(Li) detector placed successively at angles of 53°, 90°, and 140°. Values or limits were obtained for the lifetimes of 39 levels in ^{41}Ca. There is a serious disagreement between some of the lifetime values measured in the present experiment and those reported in a previous work. Accurate excitation energies and the decay scheme were also determined. Information from the lifetimes and decay scheme has been used to make spin assignments or restrictions to a number of levels in ^{41}Ca. The electromagnetic transition strengths determined from the present lifetime measurements and a previous measurement of γ-ray angular correlations have been compared to the predictions of two models of the negative parity spectrum of ^{41}Ca. In addition, an interpretation of part of the positive parity spectrum has been developed using the strong-coupling model. This calculation includes the effects of the Coriolis term in the Hamiltonian which mixes rotational bands, and the calculated excitation energies, transition rates, and pickup spectroscopic factors have been compared with experiment.

[NUCLEAR REACTIONS ^{40}Ca$(d,p\gamma)$, $E_d = 3$ MeV, measured Doppler-shift attenuation. ^{41}Ca deduced levels, τ, J, π, $B(\Lambda)$, branching ratios.]

I. INTRODUCTION

The nucleus ^{41}Ca, with only one nucleon added to a doubly closed $T = 0$ core, provides an excellent opportunity to study the coexistence of single-particle and deformed configurations. The existence of only one valence nucleon greatly reduces the numerical complexity of theoretical calculations; yet ^{41}Ca exhibits an astonishing richness of structure in its level scheme. The well-known fragmentation of the single-particle states is one example of the important role which deformed configurations play in the structure of ^{41}Ca. Although considerable progress has been made in the experimental and theoretical understanding of this nucleus, there are still many unanswered questions.

We have undertaken an experimental program to further study the structure of ^{41}Ca by means of its electromagnetic transitions. This investigation was motivated by the hope of obtaining additional experimental information concerning spin determinations and transition rates for comparison with the predictions of existing models and, possibly, for the development of new nuclear models. The present measurement of the mean lives of many levels in ^{41}Ca is intended to complement our previous γ-ray angular correlation and decay scheme measurements.[1,2]

There have been several previous measurements of nuclear lifetimes in ^{41}Ca using the Doppler-shift attenuation method (DSAM) with the ^{40}Ca$(d,p\gamma)^{41}$Ca reaction[3,4] and the ^{41}K$(p,n\gamma)^{41}$Ca reaction.[5,6] Laurent *et al.*[3,5] have measured the lifetimes of a number of levels, whereas only the two lowest $\frac{3}{2}^-$ states were studied in the other works.[4,6] The lifetimes of several high-spin states have been measured[7,8] using the recoil-distance method. In addition, the lifetimes of the 2010-[9] and 3830-keV[10] levels have been measured using direct timing techniques. A summary of other experimental studies of ^{41}Ca can be found in a previous report.[1]

Our original purpose was to measure the lifetimes of those states in ^{41}Ca which had not been previously reported. However, our first measurement of the lifetimes using the DSAM showed serious disagreement with the values reported by Laurent *et al.*,[3,5] which are the only extensive set of DSAM lifetime measurements in print. To resolve this discrepancy, we repeated our measurement with improved statistical accuracy. Our second measurement agreed with the first one and not with many of the values of Refs. 3 and 5. We have made a number of consistency tests and feel confident of the accuracy of our lifetime values.

The calculations of Gerace and Green[11] and of Federman, Greek, and Osnes[12] have provided a reasonably successful interpretation of the negative parity level scheme of ^{41}Ca. The transition strengths measured in the present work provide a further test of the applicability of these models. A number of calculations[13–17] have been made of

the positive parity level scheme, but none can adequately describe even a portion of the spectrum. For this reason, we have applied the strong coupling model[18] to predict the positive parity spectrum of ^{41}Ca. The model considers states having two nucleons in the $N=3$ oscillator shell coupled to $K=0$ and one hole in the $N=2$ shell and includes the Coriolis term in the Hamiltonian. It provides a reasonably successful interpretation of the lower portion of the positive parity level scheme and predicts the pickup spectroscopic factors rather well. On the whole, this model is more successful than previous ones for the positive parity spectrum.

In Sec. II of this report we will discuss the experimental technique, the analysis of the Doppler-shift attenuation factors, and the resulting lifetime values and decay scheme. We will discuss the additional information which the present work provides concerning spin determinations in Sec. III. Finally, in Sec. IV, we will compare several existing model calculations of ^{41}Ca with the current state of experimental knowledge and then develop a strong-coupling model interpretation of the positive parity spectrum.

II. MEASUREMENT

A. Experimental technique

Several methods of producing excited levels in ^{41}Ca were explored, including the ^{41}K(p,n), ^{39}K-$(^3$He$,p)$, and ^{40}Ca(d,p) reactions. The latter reaction at low incident energy was selected because it populates almost all the levels of interest with adequate strength, it allows use of a metallic target, and the emerging protons (unlike neutrons) can be detected with reasonably high efficiency and energy resolution. Protons from the reaction were detected in coincidence with the γ rays to restrict the cone of ^{41}Ca recoils and to determine the excitation energy of the state producing the γ ray.

The target consisted of 0.4-mg/cm^2 of natural calcium metal evaporated on a 1.3-mg/cm^2 gold backing and covered with an 0.1-mg/cm^2 layer of gold. The backing served to stop recoiling ^{41}Ca ions and both layers of gold shielded the calcium to reduce oxidation during transfer of the target to the scattering chamber. A deuteron beam energy of 3 MeV was chosen as a compromise between recoil-ion velocity and detector-damaging neutron radiation, both of which increase with the incident energy.

Protons were detected near 180° relative to the incident beam using an annular silicon surface-barrier detector with a 40-mg/cm^2 tantalum foil to prevent scattered deuterons from reaching the particle detector. A 65-cm^3 Ge(Li) detector with 2.7-keV resolution [full width at half-maximum (FWHM)] for 1.33-MeV γ rays was used as the γ detector. γ spectra were measured at angles of 53, 90, and 140° during the first run and at 53 and 140° during the second run.

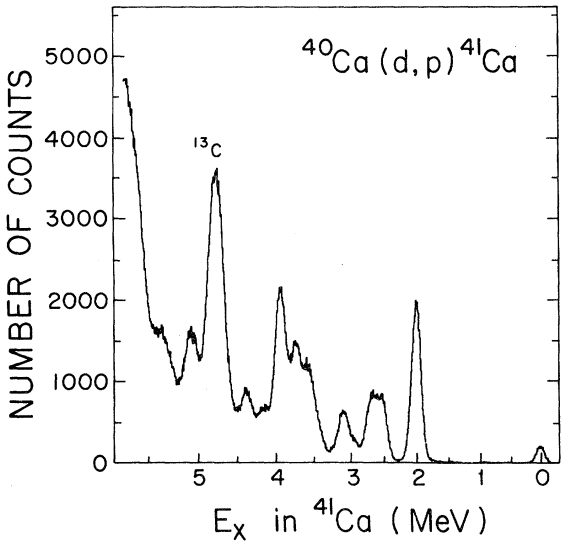

FIG. 1. The proton spectrum from the ^{40}Ca$(d,p)^{41}$Ca reaction. The approximate excitation energy in ^{41}Ca is indicated on the abscissa and the g.s. peak from the ^{12}C$(d,p)^{13}$C reaction is labeled with ^{13}C.

For each coincident event the proton energy, γ energy, and p-γ time difference signals were digitized and written on magnetic tape for off-line analysis. In addition, various live displays were generated by the computer program to monitor the progress of the experiment. The proton singles spectrum and the sampled γ singles spectrum were also accumulated and periodically written on magnetic tape. The γ singles spectrum, which included lines from several radioactive sources, served to monitor the gain stability of the system and to provide an energy calibration measured simultaneously with the data.

B. Data analysis

An energy spectrum of protons which satisfied the coincidence requirement of the slow timing circuitry (250 nsec width) is shown in Fig. 1. The particle resolution was limited by the thickness of the target and by the tantalum foil placed before the detector. The ^{12}C$(d,p)^{13}$C ground state (g.s.) peak which is labeled ^{13}C in the figure was not a source of difficulty because there are no γ rays in true coincidence with it. Spectra were accumulated of those γ rays which were in coincidence with narrow regions of the proton spectrum and whose γ-p time difference was within the true

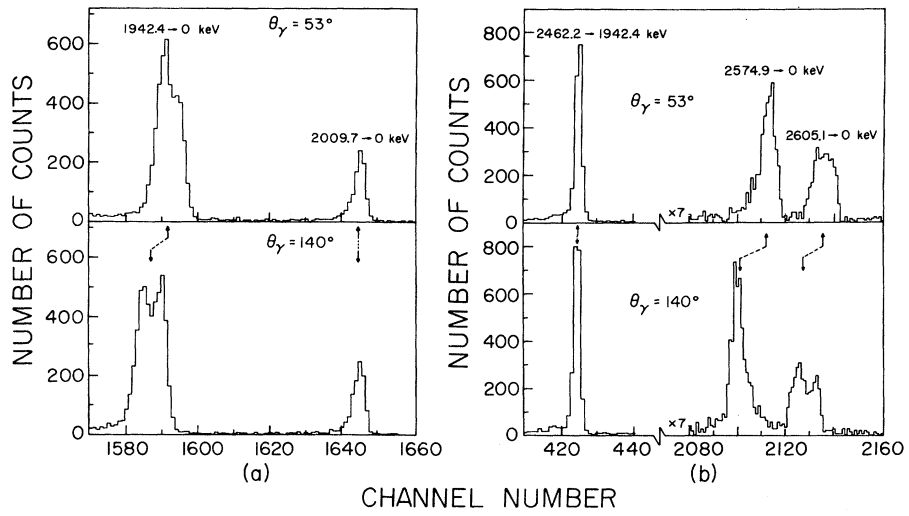

FIG. 2. Portions of the γ spectra in coincidence with two proton energy regions. The dispersion is approximately 1.22 keV/channel and the positions of the peak centroids are indicated by arrows.

coincidence peak (6 nsec FWHM). An equal-width displaced time window was used to approximately subtract random coincidences.

Portions of the γ spectra in coincidence with the proton peak near 2-MeV excitation energy are shown in Fig. 2(a). These spectra as well as the others shown in this report were accumulated during the second lifetimes measurement. No Doppler shift is visible for the γ ray from the long-lived 2010-keV state, while the 1942-keV line shows approximately 40% of the full Doppler shift. Portions of the γ spectra in coincidence with a second proton energy window can be seen in Fig. 2(b).

More examples of Doppler shifts are shown in Figs. 3 and 4. As evidenced in these figures, it was frequently possible to measure the Doppler-shift attenuation of more than one decay branch of a state. It became increasingly more difficult to measure the Doppler shifts of the states at higher excitation energy. However, some higher-lying states, such as the 4417-keV level in Fig. 4(b),

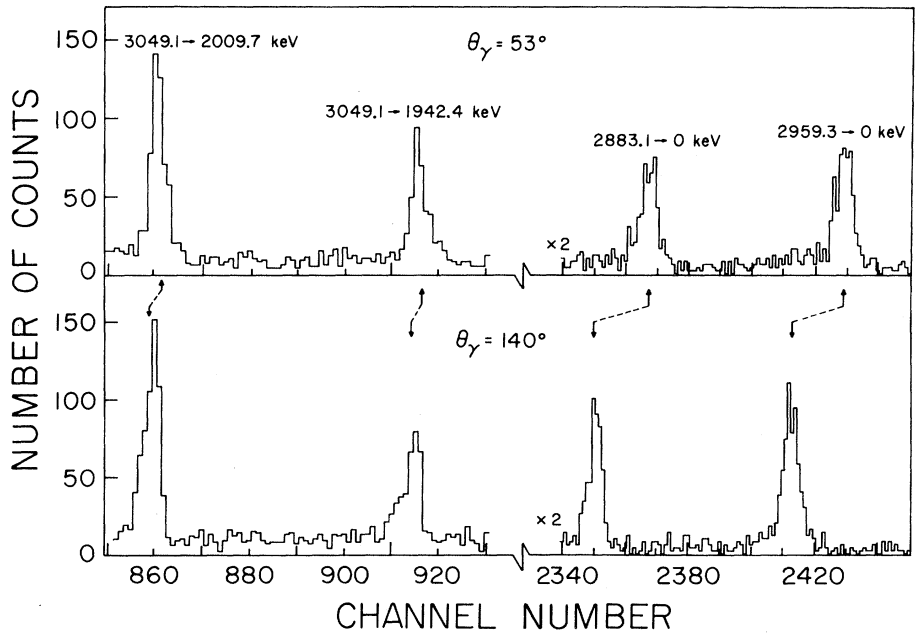

FIG. 3. Portions of the γ spectra in coincidence with one proton energy region.

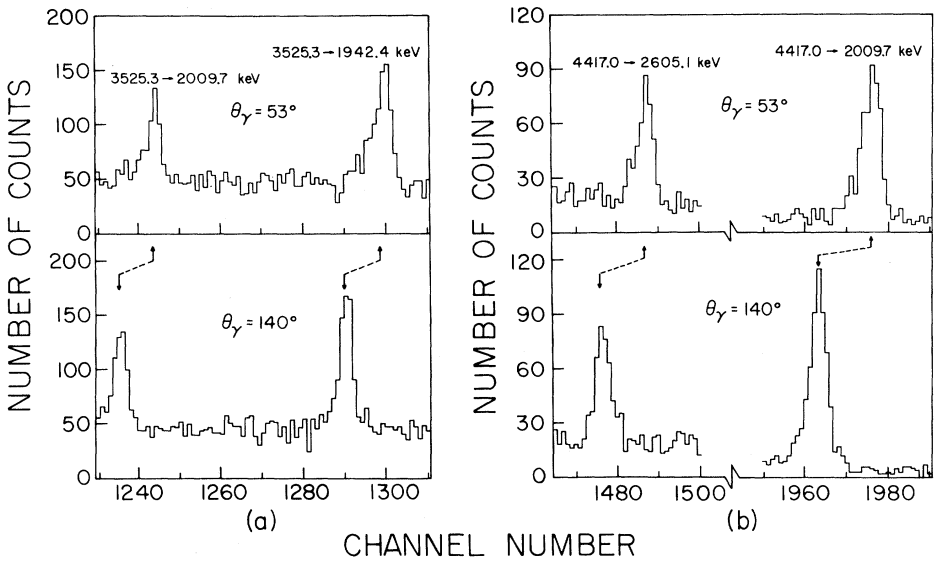

FIG. 4. Portions of the γ spectra in coincidence with two proton energy regions.

were populated strongly enough to permit an accurate measurement.

The γ-ray energies were determined from these and other spectra using peak centroid analysis. The Doppler-shift attenuation factor $F(\tau)$ was determined by least-squares fitting the γ-ray energies to a linear function of $\cos\theta_\gamma$, although such a fitting is trivial in the cases for which E_γ was measured at only two angles. The full Doppler shift can easily be calculated from the reaction kinematics because of the narrow recoil cone. The ^{41}Ca recoil velocities were about 0.005 of the velocity of light and the maximum Doppler shifts between 53 and 140° were about 0.007 of the unshifted γ-ray energy.

The electronic stopping power theory of Lindhard, Scharff, and Schiøtt[19] with the large-angle scattering considerations of Blaugrund[20] and the nuclear stopping power parametrization of Currie, Earwaker, and Martin[21] was used to infer the mean lives of the states from the attenuation of the Doppler shifts. The attenuation factor was first determined as a function of nuclear lifetime and initial recoil velocity by integrating the instantaneous ion velocity and average deflection angle over the deceleration time in the target and backing materials as well as over the point of production in the target. Then this function was numerically inverted to determine the lifetime corresponding to a measured attenuation and initial recoil velocity. The calculated electronic and nuclear stopping powers were multiplied by empirically determined[22,23] adjustment factors of 1.16 ± 0.20 and 0.7, respectively. The effect on the inferred lifetimes of the estimated ±0.20 uncertainty in electronic stopping power was added in quadrature to the uncertainties implied by the uncertainties in the measurement of $F(\tau)$ to give the final error estimate. Since the calculated lifetimes are more sensitive to the electronic than to the nuclear stopping power, we have included an uncertainty only in the former. The experimental uncertainties are dominant except for the 1942-, 2575-, and 2605-keV states where they are comparable to the uncertainty in stopping power.

C. Lifetimes

The results of the lifetime measurements are presented in Table I. The first column lists the excitation energy of each state as determined in the present work. The Doppler-shift attenuation factors $F(\tau)$ are shown separately for the two independent measurements and for all decay branches for which they could be determined reliably. Finally, the lifetimes determined from the weighted average of the attenuation factors are presented along with the results of a previous lifetime measurement.[5]

The excitation energies generally agree within errors with those quoted in the recent compilation.[24] Although he does not quote uncertainties, our excitation energies are within 1 keV of McIntyre's values[25] except for the 2575-, 3973-, 4094-, and 4279-keV levels.

The γ ray from the long-lived 2010-keV state should exhibit no Doppler shift. Therefore the measurement of the shift of this γ ray serves as a sensitive test of many sources of systematic error, and Table I shows that we are able to set a rather tight upper limit on the observed shift. The attenuation factors $F(\tau)$ in Table I for each

TABLE I. The measured Doppler-shift attenuation factors $F(\tau)$ and the mean lifetimes deduced from them.

E_I (keV)	E_F (keV)	$F(\tau)$ Run 1	$F(\tau)$ Run 2	τ (fsec) Present results	τ (fsec) Ref. 5
1942.4 ± 0.2	0	0.437 ± 0.020	0.402 ± 0.013	800 ± 70	450 ± 120 [a]
2009.7 ± 0.2	0	<0.032	<0.023	>23 000	b
2462.2 ± 0.2	1942	0.077 ± 0.032	0.087 ± 0.022	5500^{+1700}_{-1100}	>1500 [c]
2574.9 ± 0.3	0	0.742 ± 0.034	0.696 ± 0.025	260 ± 30	95 ± 30
2605.1 ± 0.3	0	0.523 ± 0.050	0.497 ± 0.034	565 ± 75	160 ± 50
2669.8 ± 0.2	1942	0.131 ± 0.044	0.119 ± 0.031	3840^{+1000}_{-700}	470 ± 140
	2010	0.116 ± 0.063	0.091 ± 0.048		
2883.1 ± 0.5	0	>0.957	0.951 ± 0.031	31 ± 24	<20
2959.3 ± 0.4	0	0.957 ± 0.042	0.924 ± 0.026	59 ± 19	<40
3049.1 ± 0.3	1942	0.228 ± 0.079	0.271 ± 0.056	1610^{+270}_{-220}	340^{+430}_{-210}
	2010	0.214 ± 0.055	0.245 ± 0.043		
3200.3 ± 0.6	0	>0.928	0.900 ± 0.046	58 ± 29	27 ± 24
3399.8 ± 0.3	2010	0.898 ± 0.055	0.834 ± 0.044	118 ± 30	
3494.7 ± 0.4	2010	0.584 ± 0.068	0.557 ± 0.069	440 ± 90	
3525.3 ± 0.3	1942	0.972 ± 0.051	0.895 ± 0.060	48 ± 24	
	2010	0.963 ± 0.060	0.942 ± 0.070		
3613.0 ± 0.6	0	>0.953	>0.969	<27	22 ± 13
3613.5 ± 0.3	1942	0.744 ± 0.066	0.711 ± 0.067	240 ± 45	
	2462	0.696 ± 0.092	0.782 ± 0.114		
	2670	0.694 ± 0.197	0.649 ± 0.186		
3675.7 ± 1.0	0	0.921 ± 0.094	0.905 ± 0.056	77 ± 40	
3730.4 ± 0.3	2462	0.624 ± 0.062	0.605 ± 0.064	370 ± 70	55 ± 20
3739.4 ± 0.3	2010	>0.915	>0.953	<46	
	2605	>0.904	>0.868		
3845.9 ± 0.6	2010	0.875 ± 0.074	0.754 ± 0.064	160 ± 45	
3943.7 ± 0.4	1942	>0.947	>0.929	<53	<25
	2462	>0.832	>0.831		
3973.3 ± 0.8	0	0.722 ± 0.264	0.876 ± 0.068	127 ± 50	
	2605	0.739 ± 0.151	0.851 ± 0.168		
4094.1 ± 0.6	0	>0.919	>0.948	<29	
	2010	>0.934	>0.937		
4184.2 ± 0.5	2010	0.938 ± 0.035	0.932 ± 0.027	56 ± 17	
	2605	<0.884	0.934 ± 0.077		
4279.0 ± 1.0	0	>0.943	>0.953	<38	
4327.5 ± 0.8	3200	>0.875	>0.835	<160	
4340.0 ± 1.2	0	0.767 ± 0.088	0.776 ± 0.057	190 ± 50	
4417.0 ± 0.4	2010	0.922 ± 0.030	0.923 ± 0.026	61 ± 14	
	2605	0.942 ± 0.053	0.951 ± 0.052		
4446.6 ± 1.8	0	>0.738	>0.825	<145	
4546.7 ± 1.0	0	0.822 ± 0.132	0.850 ± 0.058	125 ± 45	
4603.0 ± 0.5	1942	>0.922	>0.927	<54	
4728.1 ± 0.6	2010	>0.928	>0.939	<43	
4730.2 ± 0.4	1942	0.927 ± 0.047	0.915 ± 0.038	57 ± 19	
	2462	0.911 ± 0.061	>0.936		
4752.5 ± 0.4	1942	0.978 ± 0.017	0.978 ± 0.013	44 ± 15	
	2462	0.953 ± 0.026	0.945 ± 0.025		

TABLE I *(Continued)*

E_I (keV)	E_F (keV)	$F(\tau)$ Run 1	$F(\tau)$ Run 2	τ (fsec) Present results	τ (fsec) Ref. 5
4778.1± 0.5	2010	>0.958	>0.973	<22	
4813.9± 1.0	0	>0.926	>0.921	<54	
4876.2± 0.8	0	>0.966	>0.916	<49	
4969.5± 1.0	0	>0.961	>0.926	<36	
5120.1± 0.5	2670	>0.936	>0.891	<67	
5282.3± 0.5	3010	>0.947	>0.919	<53	
5411.4± 0.6	1942	>0.904	>0.957	<44	

[a] Reference 4 gives 900± 200 fsec.
[b] Reference 9 gives 0.8± 0.2 nsec.
[c] Reference 4 gives >4 psec.

state are generally consistent.

However, the mean lifetimes determined in this experiment do not agree with those of Laurent *et al.*[5] Most of the present lifetime values are larger than those of Ref. 5 and the disagreement is greatest for the states with the longest lifetimes, such as the 2670- and 3049-keV levels. The lifetime of the 1942-keV level is the one which is most accurately determined because of the high peak-to-background ratio for its γ ray and because its lifetime lies near the most rapidly changing part of the $F(\tau)$ curve. Wedberg *et al.*[4] have reported a mean life of 900± 200 fsec for this state, which is in good agreement with our value rather than with the value of 450± 120 fsec of Ref. 5. The Argonne[4] limit of >4 psec for the lifetime of the 2462-keV state is also consistent with our value and is tighter than that of Ref. 5.

The disagreement with Ref. 5 has been a principal concern in this work and was the reason for making two independent sets of measurements. We have performed several tests to verify our results including the comparison of the attenuation factors between the two measurements and the various decay branches, and we are confident of the accuracy of our lifetime values.

D. Decay scheme

We can determine approximate branching ratios for the states in ^{41}Ca by averaging those obtained at each of the three angles of observation. This average reduces the effect of γ-ray angular correlation functions on the results and improves the statistical accuracy of the ratios. The branching ratios so obtained are listed in Table II in comparison with those of McIntyre,[25] and it can be seen that the two measurements generally agree. This table includes all of the levels in Table I for which we have observed more than one decay branch. Obviously, there may be additional weak branches which we have not detected. In three cases no branching ratios are reported from this work because the strength of one branch could not be reliably measured. A few branching ratios from other sources[26,27] have been included in the table for comparison.

A summary of the ^{41}Ca level and decay scheme is shown in Fig. 5. For clarity the vertical energy scale is merely monotonic, not linear. The level scheme is fairly complete up to an excitation energy of 4 MeV. Above this energy only the states for which we were able to obtain lifetime values or limits are included, except for the 5218-keV state. In most cases the branching ratios and level energies are the results of the present measurement. The branching ratios for the 3495- and 3730-keV levels are those of McIntyre,[25] and the information about the high-spin states is taken from Refs. 7 and 8. Many of the spin assignments and restrictions in Fig. 5 will be discussed in Sec. III. The others are taken from the recent compilation of Endt and Van der Leun[24] and from Refs. 1, 7, 8, 28, and 29.

III. DISCUSSION OF INDIVIDUAL LEVELS

The results of the present experiment provide further information concerning the quantum numbers of states in ^{41}Ca. The following spin assignments or restrictions are based on the available direct reaction data together with reasonable upper limits for γ transition rates. γ-ray multipolarities of predominantly octupole or higher order are ruled out for the transitions discussed in this section. For example, a 10% γ decay branch of 5 MeV from a state with $\tau = 100$ fsec would have an $E3$ strength of 230 Weisskopf units (W.u.) or an $M3$ strength of 8700 W.u.

In the following discussion $E2$ strengths of 30 W.u. or larger have been ruled out since no $E2$ strengths greater than 5 W.u. are known in this almost closed shell nucleus. However, all $E2$ strengths below 100 W.u. which have been rejected

TABLE II. A comparison of branching ratio measurements.

E_I (keV)	E_F (keV)	Branching ratio Present	Ref. 25
2670	1942	71± 2	71± 3
	2010	29± 2	29± 2
3049	1942	26± 2	21± 2
	2010	41± 2	37± 3
	2605	30± 2	38± 3
	2670	3± 1	4± 2
3495	0		5± 2
	2010		83± 6
	3049		12± 3
3525	1942	55± 3	59± 9
	2010	35± 3	31± 5
	2670	10± 2	10± 3
3614	1942	51± 4 [a]	42± 8
	2462	33± 4 [a]	41± 9
	2670	16± 2 [a]	17± 5
3730	0		24± 4
	1942		17± 4
	2462		35± 6
	2575		24± 7
3739	2010	66± 3	67± 7
	2605	34± 3	33± 4
3846	1942	20± 5	22±13
	2010	80± 5	78±34
3944	1942	91± 3	95± 9
	2462	9± 3	5± 1
3973	0	50± 7	55±10
	2605	50± 7	45±10
4094	0	42± 5	30± 5
	2010	58± 5	70±10
4184	2010	69± 3	64±10
	2605	31± 3	36± 5
4417	2010	70± 2	
	2605	30± 2	
4730	0	18± 4	
	1942	39± 5	
	2462	43± 6	
4752	1942	67± 2	70 [b]
	2462	33± 2	30 [b]
4814	0	41± 7	
	2883	59± 7	
4970	0	42±19	
	2883	58±19	
5120	0	41±10	50±20 [c]
	2670	59±10	50±20 [c]

[a] Reference 2.
[b] Reference 26.
[c] Reference 27.

are quoted to leave the final judgment with the reader. All known $M2$ strengths in this mass region are considerably retarded[30] compared to the single-particle estimate. The one previous exception in ^{43}Ca has now been shown[31] to also be strongly retarded. Consequently we have rejected $M2$ transition rates greater than 0.8 W.u.

Among the 46 transitions between states of known parity in Fig. 5 there is only one transition from a negative parity to a positive parity state. Hence if most or all of the decay branches of a given state are to positive parity levels, that state is more likely to have positive parity. Since the confidence level of this rule is hard to estimate, such parity suggestions are enclosed in parentheses in Fig. 5.

2575-keV level. The lifetimes of the 2575- and 3731-keV levels would imply unreasonably large $M2$ strengths of 130 and 1200 Weisskopf units (W.u.) for the 2575 → 0 keV and 3731 → 2575 keV transitions, respectively, if they were purely magnetic quadrupole in character. These restrictions and the assignment[29] of $J^\pi = \frac{3}{2}^-$ to the 3731-keV level reduce the possible spin-parity values of the 2575-keV level to $\frac{3}{2}^-$, $\frac{5}{2}^\pm$, or $\frac{7}{2}^-$. The latter possible spin would imply an unlikely $E2$ strength of 30 W.u. for the 3731 → 2575 keV transition. The tentative $l=2$ assignment in the ^{41}Ca(α, α') reaction[30] would imply negative parity for this level. Altogether the most probable values are $J^\pi = \frac{3}{2}^-$ or $\frac{5}{2}^-$ for the 2575-keV level.

2605-keV level. The assignment of a mixed $l=3$ and $l=5$ angular distribution pattern in the ^{41}Ca(α, α') reaction[32] implies positive parity for this level, and its lifetime would imply an unreasonably large $M2$ strength of 55 W.u. for the 2605 → 0 keV transition. These facts restrict J^π of this level to $\frac{5}{2}^+$, $\frac{7}{2}^+$, or $\frac{9}{2}^+$. The lifetime of the 3739-keV level (assigned $\frac{3}{2}^+$ in Ref. 1) would imply an unreasonably large $E2$ strength of >350 W.u. if $J^\pi = \frac{7}{2}^+$ for the 2605-keV level and an even larger $M3$ strength for the hypothesis of $\frac{9}{2}^+$. Therefore $J^\pi = \frac{5}{2}^+$ for the 2605-keV level.

2883-keV level. The $l=2$ assignment to this level in the ^{39}K$(^3$He$, p)$ reaction[33] implies positive parity and restricts $J \leq \frac{9}{2}$. The lifetime of this level and its g.s. decay branch further restrict J^π to $\frac{5}{2}^+$, $\frac{7}{2}^+$, or $\frac{9}{2}^+$. The decay branches to this state from the 4814-keV $\frac{5}{2}^+$ and the 4971-keV $\frac{9}{2}^+$ levels would imply $E2$ strengths of >39 W.u. and >32 W.u. if $J^\pi = \frac{5}{2}^+$ or $\frac{9}{2}^+$, respectively, for the 2883-keV level. $E2$ strengths this large are very unlikely in ^{41}Ca, so that J^π is most probably $\frac{7}{2}^+$.

3049-keV level. The lifetime of this state would imply unreasonably large $E2$ transition strengths of 300 and 1300 W.u. for its decay branches to the 2670- and 2605-keV levels if its spin-parity were $\frac{5}{2}^+$ or $\frac{1}{2}^+$, respectively. The $M2$ strengths would

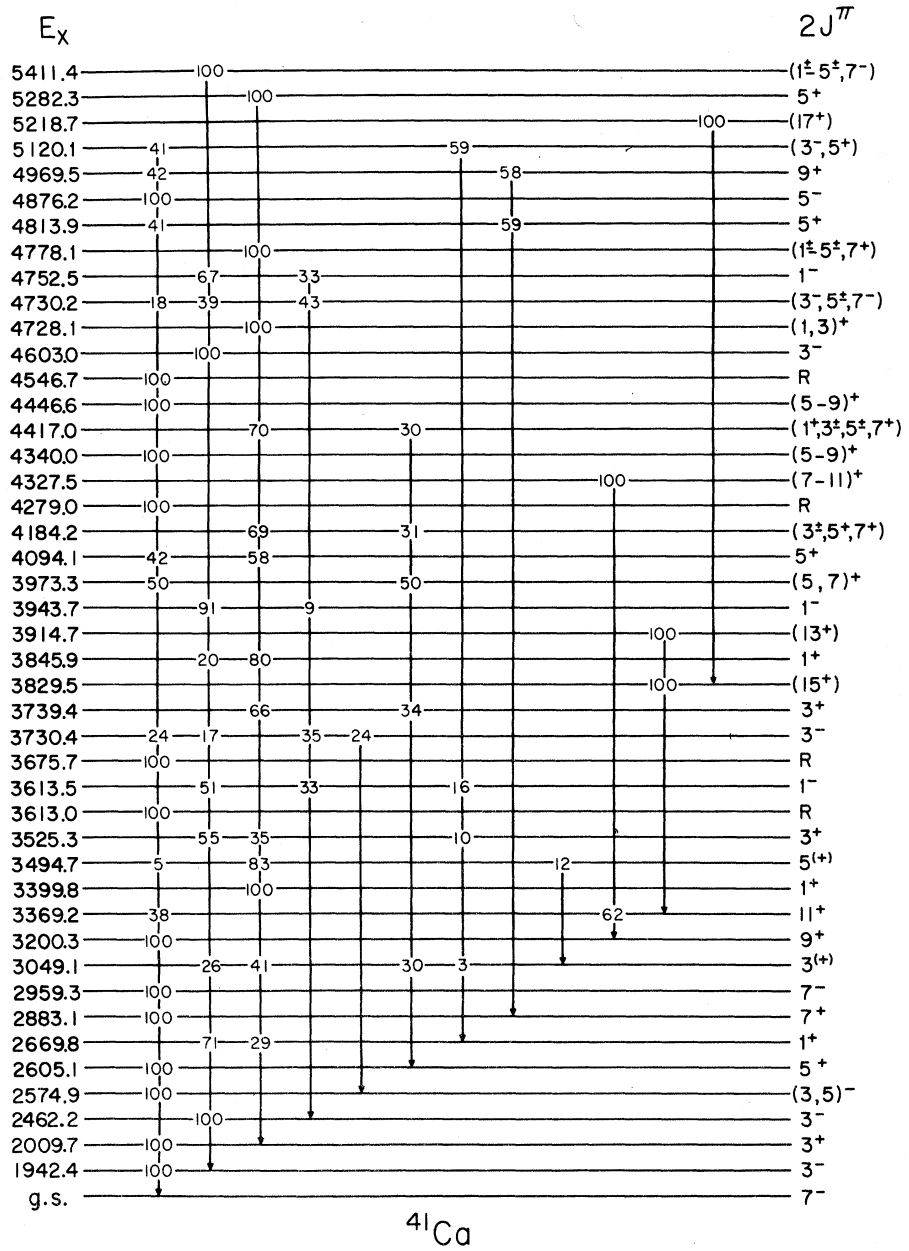

FIG. 5. A ^{41}Ca level and decay scheme. The information displayed includes results of the present as well as previous work and its sources are discussed in the text. R indicates the spin restriction $2\ J^{\pi} = (3^{-}, 5^{\pm}, 7^{\pm}, 9^{\pm}, 11^{-})$.

be even larger if $J^{\pi} = \frac{5}{2}^{-}$ or $\frac{1}{2}^{-}$. Therefore $J = \frac{3}{2}$ for the 3049-keV level. Positive parity is favored because 3 of its 4 decay branches are to positive parity levels.

3495-keV level. The l value of this level is in doubt because of a neighboring level at 3525 keV which has not been resolved[32,33] from the 3495-keV state. If $J^{\pi} = \frac{3}{2}^{+}$ for this level, then the g.s. transition would have an $M2$ strength of 0.8 W.u., which is stronger than known $M2$ strengths in this mass region. If $J^{\pi} = \frac{7}{2}^{+}$, the transition to the 3050- keV level would have an unreasonably large $E2$ strength of 1500 W.u., while $J^{\pi} = \frac{7}{2}^{-}$ would imply an even larger $M2$ strength. These arguments restrict the possible spin-parity values to $\frac{3}{2}^{-}$ or $\frac{5}{2}^{\pm}$. The low energy transitions to two positive parity levels favor positive parity which would imply $J^{\pi} = \frac{5}{2}^{+}$ for the 3495-keV level. This value would be consistent with the $l = 2$ assignment[32,33] made to one or both members of this doublet.

3613-keV doublet. A previous measurement[2] proved the existence of a closely-spaced doublet

at this energy and showed that the $\frac{1}{2}^-$ member decays to the 1942-, 2462-, and 2670-keV levels. It is evident from Table I that the $F(\tau)$ values for the branches to the 1942-, 2462-, and 2670-keV levels are similar but are different from that of the g.s. transition, which is almost fully Doppler shifted. Thus the lifetime measurement provides further proof that two states exist near this energy. The γ-ray energies also show that the two states are separated by less than 1 keV.

3973-keV level. This state is populated with an $l=5$ angular distribution in the ^{41}Ca(α, α') reaction,[32] which implies positive parity. A spin-parity of $\frac{15}{2}^+$ was suggested in that work; however, the lifetime of this state precludes purely $M2$ radiation to the g.s. and limits the possible J^π values to $\frac{5}{2}^+$, $\frac{7}{2}^+$, or $\frac{9}{2}^+$. In addition $J^\pi=\frac{9}{2}^+$ would imply an unreasonably large $E2$ strength of 80 W.u. for the 3973 → 2605 keV transition. Thus $J^\pi=\frac{5}{2}^+$ or $\frac{7}{2}^+$ for the 3973-keV level.

4094-keV level. This state is populated with $l=2$ in the ^{42}Ca(p, d) reaction,[34,35] limiting its possible spin-parity to $\frac{3}{2}^+$ or $\frac{5}{2}^+$. A tentative assignment of $\frac{5}{2}^+$ was made in Ref. 1. The lifetime limit measured in this work would imply an unreasonably large $M2$ transition strength of >40 W.u. if $J^\pi=\frac{3}{2}^+$. Therefore $J^\pi=\frac{5}{2}^+$ for the 4094-keV level.

4184-keV level. An $l=1$ assignment was made to this state in the ^{40}Ca(d,p) reaction,[36] which with its lifetime and decay branch to the 2605-keV level would imply $J^\pi=\frac{3}{2}^-$. However, this state is populated very weakly in the (d,p) reaction and the first maximum in the angular distribution is not as strong as for other $l=1$ states. In addition, the fact that this state decays only to positive parity levels tends to favor positive parity for the 4184-keV level. If this state does have positive parity, its transitions to the 2605- and 2010-keV levels would have $E2$ strengths of 55 and 25 W.u. if $J^\pi=\frac{1}{2}^+$ or $\frac{7}{2}^+$, respectively. An $E2$ strength of 55 W.u. is rather unlikely for this nucleus, so $J=\frac{3}{2}$, $\frac{5}{2}$, or $\frac{7}{2}$ if the 4184-keV level has positive parity.

4328-keV level. The $l=3$ angular distribution in the ^{41}Ca(α, α') reaction[32] implies positive parity for this state. The hypotheses $J^\pi=\frac{5}{2}^+$ or $\frac{13}{2}^+$ would imply an unreasonably large $E2$ strength of more than 300 W.u. to the 3200-keV $\frac{9}{2}^+$ level. Thus J^π is restricted to $\frac{7}{2}^+$, $\frac{9}{2}^+$, or $\frac{11}{2}^+$ and $\frac{11}{2}^+$ is the most probable since this state decays only to a $\frac{9}{2}^+$ state.

4728-4730-keV doublet. The energies of their decay γ rays prove that one state decays to the

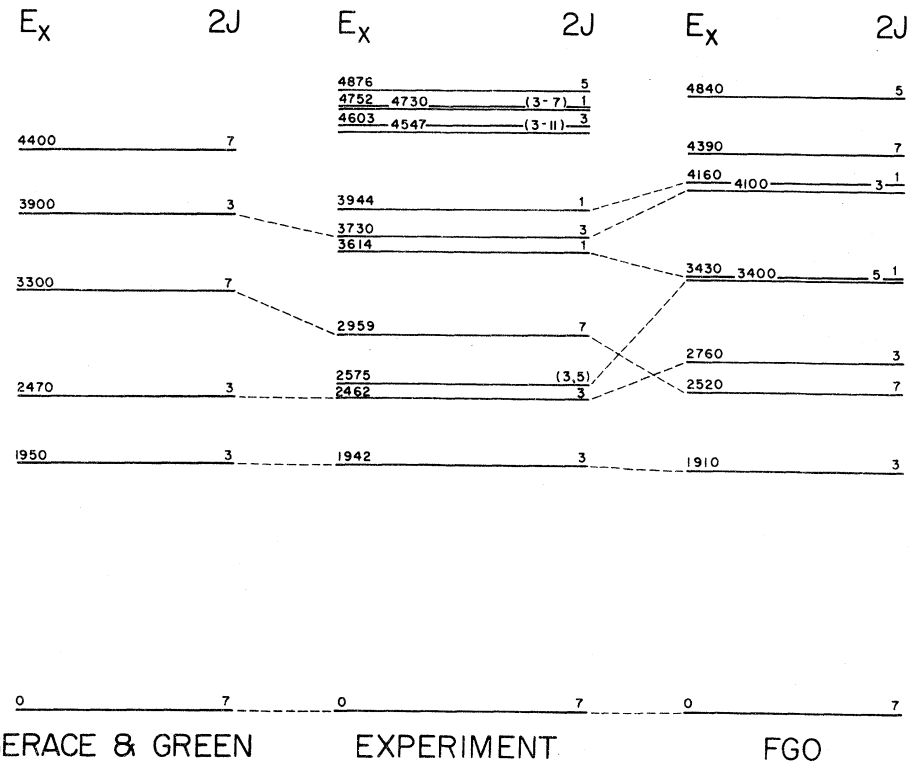

FIG. 6. A comparison of the experimental negative parity spectrum with the predictions of Gerace and Green (Ref. 11) and of Federman, Green, and Osnes (FGO) (Ref. 12).

ground, 1942-, and 2462-keV states and that another state 2 keV lower in excitation energy decays to the 2010-keV level. The decay spectrum[1] of the 6820-keV $\frac{1}{2}^+$, $T=\frac{3}{2}$ level confirms the existence of the doublet because a strong decay branch is seen to the 4728-keV level but only the 4728 → 2010 keV secondary γ ray appears in that spectrum. As discussed in Ref. 1, the 4728-keV level can probably be identified with the state seen with a predominately $l=0$ angular distribution in the ^{39}K(^{3}He, p) reaction[33] and has $J^\pi=\frac{1}{2}^+$ or $\frac{3}{2}^+$. The lifetime and decay of the 4730-keV level restrict its spin-parity to $\frac{3}{2}^-$, $\frac{5}{2}^\pm$, or $\frac{7}{2}^-$. The fact that it decays only to negative parity levels favors negative parity for this state.

4814-keV level. This state has been observed with an $l=2$ angular distribution in the ^{40}Ca(d,p)^{36} and ^{42}Ca(p, d)^{34,35} reactions; hence, $J^\pi=\frac{3}{2}^+$ or $\frac{5}{2}^+$. Its lifetime limit would imply an unreasonably large $M2$ strength of >12 W.u. for the g.s. transition if $J^\pi=\frac{3}{2}^+$. Therefore $J^\pi=\frac{5}{2}^+$ for the 4814-keV level.

5120-keV level. The lifetime of this level is too short to be consistent with predominately $M2$ or $E3$ radiation for its decay branches to either the $\frac{7}{2}^-$ g.s. or the $\frac{1}{2}^+$ state at 2670 keV. Hence, $J^\pi=\frac{3}{2}^-$ or $\frac{5}{2}^+$ and we consider $\frac{5}{2}^+$ to be more likely in view of the decay branch to the 2670-keV level.

Other levels. The g.s. decays of the following levels would have an unreasonably large $M2$ transition strength (value in parentheses) if $J^\pi=\frac{3}{2}^+$ or $\frac{11}{2}^+$: 3613 keV [$B(M2)>225$ W.u.], 3676 keV [$B(M2)=70$ W.u.], 4279 keV [$B(M2)>70$ W.u.], 4340 keV [$B(M2)=13$ W.u.], 4447 keV [$B(M2)>15$ W.u.], 4527 keV [$B(M2)=16$ W.u.]. This restricts the possible spin and parity of these levels to $\frac{3}{2}^-$, $\frac{5}{2}^\pm$, $\frac{7}{2}^\pm$, $\frac{9}{2}^\pm$, or $\frac{11}{2}^-$. In addition, the assignment of an odd l value to the 4340- and 4447-keV levels in the ^{41}Ca(α, α') reaction[32] implies that they have positive parity and $J^\pi=\frac{5}{2}^+$, $\frac{7}{2}^+$, or $\frac{9}{2}^+$.

IV. STRUCTURE OF ^{41}Ca

Perhaps the most surprising aspect of the ^{41}Ca spectrum is the abundance of levels. The level density between 2 and 5 MeV is quite high for a nucleus so near a closed shell, and it is difficult to understand all of this structure in terms of simple models.

The calculations of Gerace and Green[11] and of Federman, Greek, and Osnes[12] have provided considerable progress in the interpretation of the negative parity levels. The positive parity spectrum has previously proved less amenable to calculation. However, we have found that the strong-coupling model provides a reasonable explanation of the lower portion of the positive parity spectrum. For convenience we will discuss the interpretation of the spectrum of each parity separately.

TABLE III. A comparison of predicted and measured γ-ray transition rates among the negative parity levels of ^{41}Ca.

Transition	Ref. 11	Exp.	Ref. 12
	$B(E2)$ (e^2 fm^4)		
1942, $\frac{3}{2}^-$ → g.s., $\frac{7}{2}^-$	57	37 ± 4	77
2462, $\frac{3}{2}^-$ → g.s., $\frac{7}{2}^-$	1.2	<0.025	0.49
2959, $\frac{7}{2}^-$ → g.s., $\frac{7}{2}^-$	1.8	$5.3^{+2.7}_{-1.6}$	
3730, $\frac{3}{2}^-$ → g.s., $\frac{7}{2}^-$	2.1	0.74 ± 0.20	
	$B(M1)$ (μ_N^2)		
2462, $\frac{3}{2}^-$ → 1942, $\frac{3}{2}^-$	0.34	0.073 ± 0.018	6.6×10^{-4}
2575, $(\frac{5}{2}^-)$ → g.s., $\frac{7}{2}^-$		0.013 ± 0.002	
2959, $\frac{7}{2}^-$ → g.s., $\frac{7}{2}^-$	0.08	$0.034^{+0.016}_{-0.008}$	
3614, $\frac{1}{2}^-$ → 1942, $\frac{3}{2}^-$		0.026 ± 0.007	
3614, $\frac{1}{2}^-$ → 2462, $\frac{3}{2}^-$		0.052 ± 0.015	
3730, $\frac{3}{2}^-$ → 1942, $\frac{3}{2}^-$	0.37	0.005 ± 0.002	
3730, $\frac{3}{2}^-$ → 2462, $\frac{3}{2}^-$	0.10	0.026 ± 0.007	
3730, $\frac{3}{2}^-$ → 2575, $\frac{5}{2}^-$		0.024 ± 0.009	
3944, $\frac{1}{2}^-$ → 1942, $\frac{3}{2}^-$		>0.12	
3944, $\frac{1}{2}^-$ → 2462, $\frac{3}{2}^-$		>0.03	

A. Negative parity levels

The spectrum of levels which are known or suspected to have negative parity is shown in Fig. 6. In a few cases our selection of states for this figure has been somewhat arbitrary. The reader is referred to Sec. III and to Fig. 5 for more information concerning spin and parity assignments. The most obvious feature seen in Fig. 6 is the fragmentation of the single-particle levels. It is apparent from the outset that core excitations must play an important role.

Gerace and Green[11] have interpreted a part of this spectrum as arising from the mixing of 3p (particle in the $1f-2p$ shell) -2h (hole in the $2s$-$1d$ shell) and 5p – 4h deformed states with the $1f_{7/2}$ and $2p_{3/2}$ model states. The resulting level scheme is shown on the left in Fig. 6. Experimental counterparts have recently been identified for the second $\frac{7}{2}^-$ state[28] and the third $\frac{3}{2}^-$ state.[29] No experimental state has yet been identified with the third predicted $\frac{7}{2}^-$ state. The most likely candidates are the levels at 4279, 4547, and 4730 keV. The decay scheme of the lowest $\frac{7}{2}^-$, $T=\frac{3}{2}$ state in ^{41}Ca provides[1] an experimental measure of the amplitude of the 3p – 2h configuration in the wave

function of the second $\frac{7}{2}^-$ state relative to that in the g.s. The measured ratio of 1.6 is in qualitative agreement with the value of 2.4 predicted by this model.[11]

The electromagnetic transition rates predicted by this model are compared with the experimental values determined in the present work in Table III. We have listed the values quoted in Ref. 11 for the smaller assumed deformations. No g.s. branch has ever been observed from the 2462-keV state. The $B(E2)$ limit in Table III for this branch comes from a branching ratio limit of <1.5% determined from our γ spectra and from the measured lifetime. The $B(E2)$ value for the $\frac{7}{2}^- \rightarrow \frac{7}{2}^-$ transition results from the mixing ratio of $\delta = 0.307 \pm 0.033$ measured in Ref. 1 and the present lifetime measurement. Except for the $\frac{7}{2}^- \rightarrow \frac{7}{2}^-$ transitions, the $B(M1)$ values listed in Table III assume that the decay is purely dipole. For most cases, a reasonable $E2$ admixture would not materially reduce these values. The model of Gerace and Green tends to predict transition rates that are too fast.

Federman, Greek, and Osnes[12] (FGO) have interpreted the negative parity spectrum of ^{41}Ca in a weak-coupling picture. Specifically, their model involves coupling the $1f_{7/2}$, $2p_{3/2}$, $2p_{1/2}$, and $1f_{5/2}$ shell model states to the g.s. and the first three members of the lowest $K^\pi = 0^+$ rotational band in ^{40}Ca. The levels predicted by this model below 5 MeV are shown on the right in Fig. 6. The first two $\frac{7}{2}^-$ levels and the first three $\frac{3}{2}^-$ levels presumably correspond to the same experimental levels as those predicted by Gerace and Green. Now that conflicts with the assignment of $J^\pi = \frac{1}{2}^-$ to the 3614-keV level have been resolved,[2] it is clear that the two lowest $\frac{1}{2}^-$ states in the FGO model correspond to the 3614- and 3944-keV levels. The lowest predicted $\frac{5}{2}^-$ state may correspond to the 2575-keV level. Although the second predicted $\frac{5}{2}^-$ state could correspond to the 4876-keV level, there is a large disparity between predicted ($S = 0\%$) and measured ($S = 12\%$) spectroscopic factors for this state in the ^{40}Ca(d, p) reaction.

The γ-ray transition rates calculated by FGO are included in Table III. The $E2$ strength of the lowest $\frac{3}{2}^- \rightarrow \frac{7}{2}^-$ transition is predicted about twice as strong as the measured value and the $\frac{3}{2}^-(2) \rightarrow$ g.s. $E2$ strength is predicted to be retarded but not as much as is observed. The FGO prediction for the $\frac{3}{2}^-(2) \rightarrow \frac{3}{2}^-(1)$ $M1$ strength is far too low.

B. Positive parity levels

The spectrum of levels in ^{41}Ca known or suspected to have positive parity is shown in Fig. 7. In some cases our selection of states for this figure has been somewhat arbitrary and a few levels of uncertain parity have been included in both Fig. 6 and Fig. 7. We would again refer the reader to Sec. III and Fig. 5 for more information concerning spins and parities. Much of the $1d_{3/2}$ and $2s_{1/2}$ spectroscopic strength in the neutron pickup reactions[34,35] on ^{42}Ca is concentrated in the 2010- and 2670-keV states. The energy spacing of 660 keV between these states is much closer than that of the corresponding hole states in ^{39}Ca and ^{39}K, which is about 2.5 MeV. This reduction in spacing is one of the features that a successful model would hopefully explain.

A number of attempts have been made to predict the positive parity level scheme of ^{41}Ca. Among the shell model calculations some[14,15] have considered only $(1f_{7/2})^2(1d_{3/2})^{-1}$ configurations, while that of Sartoris and Zamick[16] included all $(1f\text{-}2p)^2$ $(2s_{1/2}\text{-}1d_{3/2})^{-1}$ configurations. None of these calculations has predicted a level density which is more than a fraction as high as that seen in the experimental spectrum. The proximity of the experimental states with large $d_{3/2}$ and $s_{1/2}$ pickup spectroscopic strength shows the importance of considering both $d_{3/2}$ and $s_{1/2}$ hole configurations. However the model of Sartoris and Zamick, which includes both hole states, fails to predict a $\frac{1}{2}^+$ state with a large $(s_{1/2})^{-1}$ component close enough to the lowest $\frac{3}{2}^+$ state.

Somewhat more successful is the phonon-particle coupling model of Goode and Zamick,[17] whose predicted levels below 5 MeV (for one choice of single-particle energies) are shown in Fig. 7. Although the lowest $\frac{1}{2}^+$ and $\frac{3}{2}^+$ states are predicted too high, their spacing is close to the experimental value. Some states of higher spin appear below 5 MeV, but there are still many features of the ^{41}Ca positive parity spectrum, such as the large number of levels, which are not accounted for in this model.

Seth, Saha, and Greenwood[37] have suggested the existence of a $K^\pi = \frac{3}{2}^+$ rotational band in ^{41}Ca whose inertial energy constant $\hbar^2/2\mathcal{I}$ of 40 keV is less than the rigid body value of 60 keV. However, the 3676-keV state, which is suggested to be the $\frac{11}{2}^+$ member of this band, has a lifetime too short to be consistent with an $M2$ g.s. decay. So J^π cannot be $\frac{11}{2}^+$ for this state.

There is some justification for considering ^{41}Ca as a deformed rotor in spite of its proximity to a closed shell nucleus. The success of the models of Gerace and Green[11] and FGO[12] demonstrates the importance of deformed configurations in the negative parity spectrum. One might reasonably expect a larger deformation among the positive parity levels which involve 2p-1h and higher configurations. ^{43}Ca, with just 2 neutrons more than

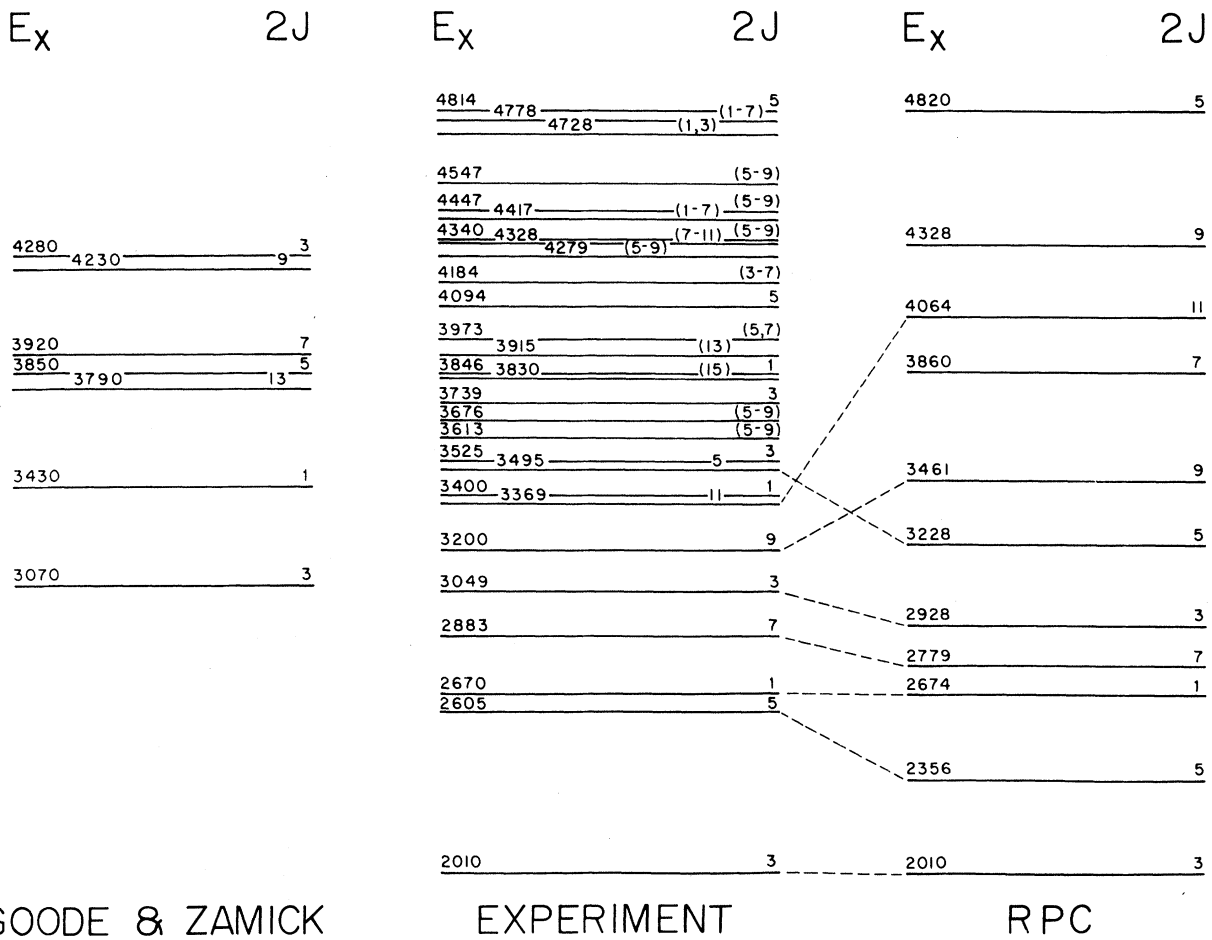

FIG. 7. A comparison of the experimental positive parity spectrum with the predictions of Goode and Zamick (Ref. 17) and of the strong coupling model (RPC).

^{41}Ca, has a distinct $K^{\pi}=\frac{3}{2}^{+}$ rotational band.[38] There are some suggestions of rotational bands in Fig. 7, but none has an energy spacing which is proportional to $J(J+1)$.

Because of these suggestions of rotational bands, we have performed some calculations to test the applicability of the strong-coupling model[18] to the positive parity spectrum of ^{41}Ca. Only those states which have two particles in the $N=3$ oscillator shell coupled to $K=0$, $T=1$ and one hole in the $N=2$ shell have been treated. However, states of good isospin have been constructed and the effect of the Coriolis term which mixes rotational bands has been included in the calculation. Since a similar model treating particles and holes in the $N=3$ oscillator shell has been discussed in a previous communication[39] we will present only a brief outline here.

The first step in the calculation involves the diagonalization of the Nilsson single-particle Hamiltonian

$$H_p=-\frac{\hbar^2}{2M}\Delta+\tfrac{1}{2}M\omega_0(r^2+\tfrac{2}{3}\delta r^2-2\delta z^2)$$
$$-\hbar\omega_0\chi(2\vec{l}\cdot\vec{s}+\mu\vec{l}\cdot\vec{l})$$

in a basis of harmonic oscillator states. This determines the energies and wave functions of the intrinsic states in the $N=2$ oscillator shell. An example of a state in ^{41}Ca with good isospin constructed by filling these Nilsson states with nucleons is shown in Fig. 8.

The next step is the diagonalization of the total Hamiltonian

$$H=\frac{\hbar^2}{2\mathcal{I}}(I^2-2\vec{I}\cdot\vec{j}+j^2)+E_p$$

in a basis of Nilsson states. E_p is the Nilsson single-particle energy and

$$-\frac{\hbar^2}{\mathcal{I}}(\vec{I}\cdot\vec{j})$$

is the Coriolis term which couples rotation and

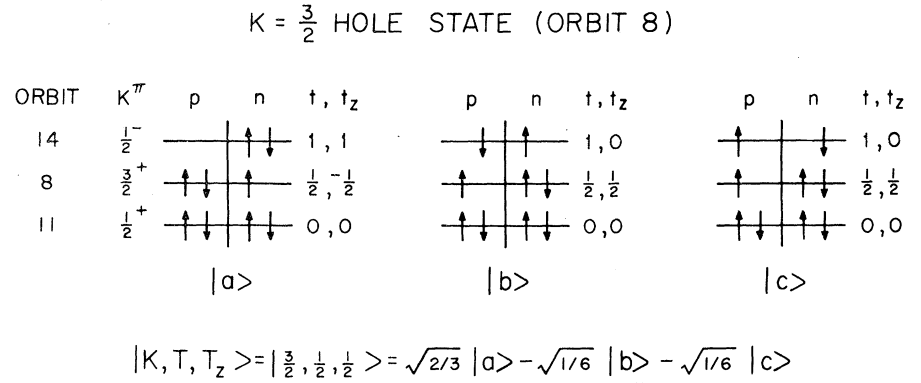

FIG. 8. An example of a positive parity Nilsson state with good isospin in ^{41}Ca. The diagrams illustrate the distribution of nucleons into the highest $N=2$ and the lowest $N=3$ Nilsson orbits. The orbits with energies lower than those shown are assumed to be filled. The arrows represent nucleons with angular momentum components $+K\hbar$ or $-K\hbar$ along the body-fixed z axis.

particle motion (RPC) and mixes the rotational bands built on the different intrinsic states. Of course, after this mixing, the state illustrated in Fig. 8 becomes only one component in the wave function of a given state.

Reasonable values have been chosen for the adjustable parameters in this model. We have used the Nilsson values[18] of $\chi=0.05$ and $\hbar\omega_0=41A^{-1/3}$. The over-all energy scale was adjusted to give the lowest $\frac{3}{2}^+$ state an excitation energy of 2.01 MeV. The value of $\mu=0.22$ was chosen to place the lowest $\frac{1}{2}^+$ state at approximately 2.67 MeV. This value of μ lies between the values of 0 and 0.35 used by Nilsson for the $N=2$ and $N=3$ oscillator shells. A value of 0.2 was used for the deformation parameter δ. Finally we have used 75 keV for the inertial parameter $\hbar^2/2\mathcal{I}$, a value deduced from the nearest nucleus with a distinct rotational band,[38] ^{43}Ca.

The levels predicted below 5 MeV are shown in Fig. 7 for comparison with experiment. Dashed lines are drawn to indicate the probable correspondence between predicted and experimental levels. The second predicted $\frac{7}{2}$ and $\frac{9}{2}$ states may correspond to the 3613- and 3676-keV levels, although not necessarily respectively. This model does successfully predict the lower-lying levels in Fig. 7. However, it predicts high-spin states at too high an energy and does not predict as many states as are observed. In fact, the successes and failures of the model for ^{41}Ca are not so different from those encountered in the mid-$f_{7/2}$ shell for such nuclei as ^{47}Ti,[40] ^{49}V,[41] and ^{49}Cr.[39]

One obvious limitation of this model is the requirement that the two nucleons in the $N=3$ oscillator shell be coupled to $K=0$, $T=1$. Configurations involving the recoupling of these nucleons may account for many of the observed levels which are not predicted by the present model.

A further test of the model is the comparison of the predicted spectroscopic factors for the ^{42}Ca(p, d) reaction with experiment. In this model the pickup spectroscopic factor to a positive parity state of total spin I is given[39,42] by

$$\left(\sum_n \sqrt{\tfrac{4}{3}}\, a_n c^n_{jK}\right)^2 \quad \text{for } j=I.$$

The sum extends over all Nilsson states that are

TABLE IV. A comparison of predicted and measured spectroscopic factors for the ^{42}Ca$(p,d)^{41}$Ca reaction.

^{41}Ca level	RPC	Ref. 34	Ref. 35	Ref. 43
2010, $\frac{3}{2}^+$	1.62	2.7	3.0	2.1
2605, $\frac{5}{2}^+$	0.06			
2670, $\frac{1}{2}^+$	0.88	0.34	0.70	0.56
3049, $\frac{3}{2}^+$	0.32			
3495, $\frac{5}{2}^+$	0.19	0.31[a]	0.34[a]	0.07
4094, $\frac{5}{2}^+$	1.71	0.49	0.48	0.20
4814, $\frac{5}{2}^+$		0.11	0.16	0.10

[a] Not resolved from the 3525-keV level.

TABLE V. A comparison of predicted and measured $M1$ transition rates among the positive parity levels of ^{41}Ca. The units are $\mu_N{}^2$.

Transition	Exp.	RPC
2670, $\frac{1}{2}^+ \rightarrow$ 2010, $\frac{3}{2}^+$	0.015 ± 0.003	0.002
3049, $\frac{3}{2}^+ \rightarrow$ 2010, $\frac{3}{2}^+$	0.012 ± 0.002	0.000
3049, $\frac{3}{2}^+ \rightarrow$ 2605, $\frac{5}{2}^+$	0.117 ± 0.020	0.032
3049, $\frac{3}{2}^+ \rightarrow$ 2670, $\frac{1}{2}^+$	0.019 ± 0.007	0.001
3369, $\frac{11}{2}^+ \rightarrow$ 3200, $\frac{9}{2}^+$	0.248 ± 0.027	0.077
3495, $\frac{5}{2}^+ \rightarrow$ 2010, $\frac{3}{2}^+$	0.033 ± 0.009	0.040
3495, $\frac{5}{2}^+ \rightarrow$ 3049, $\frac{3}{2}^+$	0.175 ± 0.063	1.238

admixed in the wave function of the final state. The amplitudes of these admixtures are represented by a_n, while the coefficients c^n_{jK} represent the amplitudes of the spherical states $|j\rangle$ in the nth Nilsson state with intrinsic axis spin projection K. The factor $\sqrt{\frac{4}{3}}$ gives the amplitude for formation of the $T_<$ state and the neutron occupation amplitude.

Some predicted spectroscopic factors are compared with the experimental values[34,35,43] in Table IV. Since the maximum intrinsic spin in the $2s$-$1d$ shell is $\frac{5}{2}$, this model predicts a zero spectroscopic factor for any state with spin greater than $\frac{5}{2}$. Of course, such states can be populated by multistep processes or through other components in the ^{42}Ca g.s. wave function. The agreement between predicted and measured spectroscopic factors is reasonably good. Specifically, the 2010- and 2670-keV levels are predicted and observed to have considerable spectroscopic strength, while the 2605-, 3049-, and 3495-keV levels are predicted and observed to be weaker in the pickup reaction. The position and spectroscopic strength of the lowest predicted $\frac{1}{2}^+$ state is a direct result of strong mixing among the three $K=\frac{1}{2}$ states in the $N=2$ oscillator shell. The lowest $\frac{1}{2}^+$ state has predominantly a hole in the Nilsson orbit No. 11. The effect of the deformation is to admix a significant amount of the spherical $s_{1/2}$ state into the wave function of orbit No. 11 without drastically shifting its energy. The result is a $\frac{1}{2}^+$ state close to the $\frac{3}{2}^+$ state which carries a considerable $s_{1/2}$ pickup strength.

A single state at 4820 keV is predicted to carry most of the $(1d_{5/2})^{-1}$ spectroscopic strength, but there appears to be no single experimental state which corresponds to it. The placement of the predicted value of the spectroscopic factor between two experimental states in Table IV is intended to indicate the possibility of fragmentation of the model state as well as the uncertainty in determining an experimental counterpart.

The electromagnetic transition strengths among the positive parity levels, which have been measured in the present work, can also be compared with the predictions of the strong coupling model. We have used the expressions of Brockmeier *et al.*[44] to calculate transition rates in this model. The free nucleon charges and magnetic moments were used, while a gyromagnetic ratio of $g_R = Z/A$ was assumed for the core. A comparison of predicted and measured $M1$ transition rates is presented in Table V. The agreement is not very good, but this model is generally less successful in predicting $M1$ transition rates. The γ transition rates provide further evidence that the observed high-spin states are not described well by this model. The $E2$ strength of the $\frac{15}{2}^+ \rightarrow \frac{11}{2}^+$ transition is measured[7,8,10] to be about 1 W.u., whereas the model predicts a 15-fold enhancement.

In summary, the strong-coupling model predicts, with reasonable success, the lower portion of the positive parity spectrum of ^{41}Ca. For these states, it reproduces the energy spacing and spectroscopic factors rather well. The model is less successful in predicting $M1$ transition rates and the energy spacing of the high-spin states. It also fails to account for perhaps one-half of the positive parity states.

We hope that the improved experimental knowledge of ^{41}Ca will stimulate further theoretical study of this nucleus.

ACKNOWLEDGMENTS

The authors are grateful to W. J. Gerace for providing unpublished γ transition rate calculations and are pleased to acknowledge informative discussions with P. Federman, W. J. Gerace, and S. Pittel.

---

†Work supported by the National Science Foundation.

[1]S. L. Tabor, R. W. Zurmühle, and D. P. Balamuth, Phys. Rev. C 11, 1089 (1975).
[2]S. L. Tabor, R. W. Zurmühle, and D. P. Balamuth, Phys. Rev. C 8, 2200 (1973).
[3]H. Laurent, S. Fortier, J. P. Schapira, R. S. Blake, F. Picard, and J. Dalmas, Nucl. Phys. A164, 279 (1971).
[4]G. H. Wedberg, G. B. Beard, R. C. Bearse, and R. E. Segel, Bull. Am. Phys. Soc. 15, 601 (1969).
[5]H. Laurent, S. Fortier, J. P. Schapira, A. Huck, and G. Walter, Nucl. Phys. A164, 289 (1971).
[6]R. E. Segel, R. H. Siemssen, S. Baker, and A. E. Blaugrund, Phys. Rev. 158, 1063 (1967).
[7]K. P. Lieb, M. Uhrmacher, J. Daub, and A. M. Kleinfeld, Nucl. Phys. A223, 445 (1974).
[8]P. Gorodetzky, J. J. Kolata, J. W. Olness, A. R. Poletti, and E. K. Warburton, Phys. Rev. Lett. 31, 1067 (1973).
[9]R. E. Holland and F. J. Lynch, Phys. Rev. C 2, 1365 (1970).
[10]H. J. Kim, R. L. Robinson, and W. T. Milner, Phys. Rev. C 11, 1468 (1975).
[11]W. J. Gerace and A. M. Green, Nucl. Phys. A93, 110 (1967); W. J. Gerace (private communication).
[12]P. Federman, G. Greek, and E. Osnes, Nucl. Phys. A135, 545 (1969).
[13]A. E. L. Dieperink and P. J. Brussaard, Nucl. Phys. A106, 177 (1968).
[14]A. Armigliato, L. M. El-Nadi, and F. Pellegrini, Nuovo Cimento 498, 142 (1967).
[15]C. T. Chen-Tsai, S. T. Hsieh, and T. Y. Lee, Phys.

Rev. C 4, 2096 (1971).
[16]G. Sartoris and L. Zamick, Phys. Rev. Lett. 18, 292 (1967).
[17]P. Goode and L. Zamick, Nucl. Phys. A129, 81 (1969).
[18]S. G. Nilsson, K. Dan. Vidensk. Selsk. Mat.-Fys. Medd. 29, No. 16 (1955).
[19]J. Lindhard, M. Scharff, and H. E. Schiøtt, K. Dan. Vidensk. Selsk. Mat.-Fys. Medd. 33, No. 14 (1963).
[20]A. E. Blaugrund, Nucl. Phys. 88, 501 (1966).
[21]W. M. Currie, L. G. Earwaker, and J. Martin, Nucl. Phys. A135, 325 (1969).
[22]A. E. Blaugrund, D. H. Youngblood, G. C. Morrison, and R. E. Segel, Phys. Rev. 158, 893 (1967).
[23]R. A. I. Bell, J. L'Ecuyer, R. D. Gill, B. C. Robertson, I. S. Towner, and H. J. Rose, Nucl. Phys. A133, 337 (1969).
[24]P. M. Endt and C. Van der Leun, Nucl. Phys. A214, 1 (1973).
[25]L. C. McIntyre, Phys. Rev. C 9, 200 (1974).
[26]H. Gruppelaar and P. Spilling, Nucl. Phys. A102, 226 (1967).
[27]S. Fortier, H. Laurent, and J. P. Schapira, J. Phys. 32, 231 (1971).
[28]K. K. Seth, A. Saha, W. Stewart, W. Bennenson, W. A. Lanford, H. Nann, and B. H. Wildenthal, Phys. Lett. 49B, 157 (1974).
[29]K. K. Seth and S. G. Iverson, Phys. Lett. 53B, 171 (1974).
[30]D. Kurath and R. D. Lawson, Phys. Rev. 161, 915 (1967).
[31]S. L. Tabor, D. P. Balamuth, and R. W. Zurmühle, Bull. Am. Phys. Soc. 19, 1034 (1974).
[32]M. J. A. de Voigt, D. Cline, and R. N. Horoshko, Phys. Rev. C 10, 1798 (1974).
[33]T. A. Belote, F. T. Dao, W. E. Dorenbusch, J. Kuperus, J. Rapaport, and S. M. Smith, Nucl. Phys. A102, 462 (1967).
[34]S. M. Smith, A. M. Bernstein, and M. E. Rickey, Nucl. Phys. A113, 303 (1968).
[35]P. Martin, M. Buenerd, Y. duPont, and M. Chabre, Nucl. Phys. A185, 465 (1972).
[36]T. A. Belote, A. Sperduto, and W. W. Buechner, Phys. Rev. 139, B80 (1965).
[37]K. K. Seth, A. Saha, and L. Greenwood, Phys. Rev. Lett. 31, 552 (1973).
[38]N. G. Alenius, S. E. Arnell, Ö. Skappstedt, E. Wallander, and Z. P. Sawa, Nuovo Cimento 8A, 147 (1972).
[39]R. W. Zurmühle, D. A. Hutcheon, and J. J. Weaver, Nucl. Phys. A180, 417 (1972).
[40]J. J. Weaver, M. A. Grace, D. F. H. Start, R. W. Zurmühle, D. P. Balamuth, and J. Noé, Nucl. Phys. A196, 269 (1972).
[41]S. L. Tabor and R. W. Zurmühle, Phys. Rev. C 10, 35 (1974).
[42]B. Elbek and P. O. Tjøm, Adv. Nucl. Phys. 3, 259 (1969).
[43]K. K. Seth, A. K. Saha, W. Stewart, W. A. Lanford, W. Beneson, and B. H. Wildenthal, Bull. Am. Phys. Soc. 19, 522 (1974).
[44]R. T. Brockmeier, S. Wahlborn, E. J. Seppi, and F. Boehm, Nucl. Phys. 63, 102 (1965).